A Radio-Source Tracker

Erwan Rouillé[(1)], Baptiste Cecconi [(1)], Boris Segret [(2)]

[(1)] LESIA, Paris Observatory, PSL University, Sorbonne University, Paris University, CNRS, 5 pl. Jules Janssen – 92195 Meudon Cedex, France, +33 1 45 07 77 01, erwan.rouille@obspm.fr

[(2)] CENSUS, Paris Observatory – PSL, 5, pl. Jules Janssen – 92195 Meudon Cedex, France, +33 1 45 07 78 24, boris.segret@observatoiredeparis.psl.eu

Abstract

The development of satellite swarm technology offers new possibilities for space studies and comes with new challenges. Among them is the need of knowledge on the swarm topology and attitude, especially in the context of space-based radio interferometry. This paper presents an algorithm that recovers the absolute swarm attitude without the help of external systems such as GNSS (Global Navigation Satellite Systems), as part of NOIRE (Nanosatellite pour un Observatoire Interferométrique Radio dans l'Espace) concept study. This algorithm uses the imaging capability of a low frequency radio interferometer in order to function like a star-tracker using the main radio sources in the sky. The Lost-In-Space (LIS) mode is presented in this paper. The Tracking mode is yet to be developed. This algorithm is studied through numerical simulations. This concept is applied here to the kilometric wavelength spectral range (30 kHz-1 MHz) but the technique can be expanded to higher frequencies. Images are reconstructed using an iterative Discrete Fourier Transform (DFT) at two frequencies and using source subtractions. Pattern-matching is run with a voting system implemented on geometrical parameters defined by triangles of sources. The radio sky at low frequency is modelled by extrapolating from sky observed at 50 MHz. The accuracy on the recovered swarm attitude is measured for different levels of noise in the interferometric visibilities. The simulation shows that the suggested pipeline can achieve an attitude knowledge error lower than 1 arcmin for a swarm scale of 100 km. The requirements in terms of memory and computation capability are discussed as well as the limitations of the technique and the simulation.

1 Introduction

Nanosatellites have known an exponential development over the last decades. Their uses went from being a concept marginally developed in universities by students to being a building block for new space technologies. Nowadays, nanosatellites can be found either in demonstration missions, either in constellation for commercial purposes or even in scientific missions.

The NOIRE concept study [1] anticipates a scientific observatory composed of a swarm of 50 nanosatellites orbiting the Moon. It is meant to observe the sky at extremely low frequency (30 kHz-100 MHz). The sky remains mostly unexplored in this frequency range and various science cases can be covered by those wavelengths. Namely: space weather, stellar studies, planetary emissions and cosmology.

NOIRE aims to take images of the sky in this frequency range. For that, it implements the interferometry technique made possible in space thanks to swarm technologies. Each nanosatellite is equipped with antennas receiving the radio signals of interest from all directions at once. Then, the saved signals are shared and compared among the satellites of the swarm. Images can be reconstructed using the correlations between the signals and the positions of the satellites. The interferometry technique is not in the scope of this article. Yet, in order to perform interferometric measurements, the 3D topology of the swarm must be known precisely.

Recent studies for swarm of satellites choose to benefit from GNSS (Global Navigation Satellite Systems) for positioning which enable to reconstruct the full 3D topology. An example of that is the mission SunRISE (Sun Radio Interferometer Space Experiment) [2]. However, this method no longer holds for a swarm orbiting the Moon. The swarm of NOIRE is designed to be autonomous, i.e. it cannot benefit from any external supporting infrastructure. The relative 3D topology of a swarm can be retrieved with algorithms whose inputs are the distances between the satellites [4-6]. These distances can be measured autonomously. However, the topology reconstructed that way is only relative to the swarm. It means that the vectors of the position are expressed in an arbitrary frame generated by the algorithm. On the other hand, the position of the elements of interest for the observatory, namely the radio sources, are known in a different frame called the absolute frame. The transform between the two frames can be expressed as a rotation but can also include a symmetry. While the interferometer is able to generate image of the full sky, it is necessary to know this transform in order to provide directional information associated with the image.

In the previous study [1], it has been highlighted that an accuracy on the directional information provided by the instrument close to 1 arcminute is sufficient to cover all science cases.

This paper presents an algorithm that recovers the absolute swarm attitude by taking advantage of the imaging capability of the interferometer. The basic principle remains the same as a classical star-tracker. When the tracker is in *Lost-In-Space* mode (LIS), it compares the positions of recognizable patterns of the sky between the measurements and a known catalog.

The present algorithm is evaluated for the LIS mode through a numerical simulation in the context of NOIRE.

2 Methods

2.1 Pipeline

The main algorithm can be decomposed in a series of functions which are algorithms on their own. To avoid confusion, the main algorithm is called pipeline. The Structured Analysis and Design Technique (SADT) of the pipeline is detailed in Figure 1. These functions' purposes are the same as for a classical star-tracker. Only the first (A1) is specific to an interferometer.

N

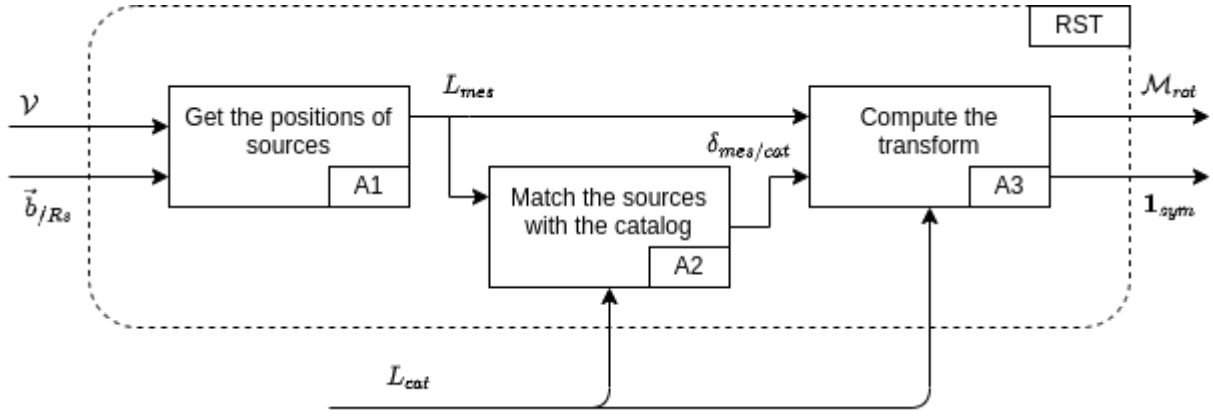

Figure 1: SADT (Structured Analysis and Design Technique) diagram of the function to be performed by the pipeline

2.2 Main differences with classical star-tracker

The images made with an interferometer are the result of a computation with the signals received by each satellite. Thus, extra steps are necessary to generate an image whereas classical star-tracker uses images coming directly from a camera.

One of the main properties of the sky at very low frequency is the limited number of bright sources. These few sources are very bright relatively to the others making it hard to find the dimmer ones. Indeed, the interferometric images contain artifacts that depends on the brightness distribution and the instrumental response. Also, these sources are scattered around the whole celestial sphere. In order to get as much of sources as possible in the images of the instrument, it is necessary to image the whole celestial sphere.

On the other hand, imaging the full sky requires a large number of pixels and thus more computation. For the sake of the simulation, the images were generated at the lowest frequencies (<1MHz) where the resolution is the lowest in order to reduce the amount of pixels and thus the computation time.

This also means that the scale of the patterns is too large to consider in their 2D projections. All distances considered on the celestial sphere are expressed as angular deviations.

Moreover, the transform between the two frames can include an unknown symmetry. Thus, all methods are implemented so that their parameters are independent of a possible symmetry.

2.3 Selecting sources

The pipeline's images are generated using the HEALPix framework [6]. The pixelization of this

framework guarantees that each pixel covers the same surface of the sky which is suited for full sky imaging (pixels coordinates are expressed in spherical coordinates(θ, ϕ)).

Once an image is generated, the first step consists in finding the main sources and storing their positions in a list. However, interferometric images are the result of a reconstruction that is incomplete, hence they contain various artifacts. These artifacts may be confused with actual sources. Detections of artifacts are called false detections. They are concerning because they may outnumber the actual sources and prevent the pipeline from working. A rejection criterion is thus applied to prevent the algorithm from adding artifacts to the list of measured positions. The criterion verifies that the candidate sources follow the instrumental response of a point source.

The selection is performed iteratively by decreasing brightness. In the simulation, the number of iterations is set to 20. Hence no more than 20 sources over the whole sky can be used for the computation.

2.4 Pattern Match

The goal of the pattern match function is to draw the link between the measured sources and the ones from the catalog in order to compute the rotation that links them.

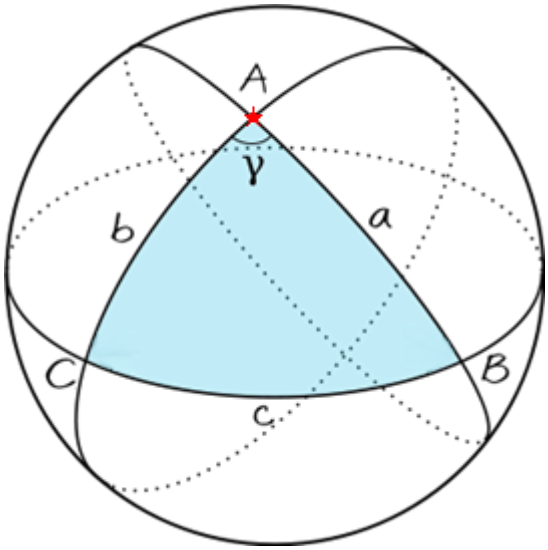

Figure 2: Parameters used to characterize the the source A (a,b,γ)

The pattern match function compares geometrical parameters formed by the sources positions between the measured ones and a catalog. The geometrical parameters implemented here are based on triangles of sources. The tables have 3 entries per source per triangle, the angular distances between the source of interest and the two others $(a, b)$and the bi-angle at the corner of the source of interest (γ). These parameters are depicted on Figure 2. Similar parameters for 2D images were used by Liebe C. [7]. Although, parameters defined by pairs of sources can be sufficient for classical star-tracker, triangles are more robust when the number of sources is low.

$$\gamma = \frac{\cos(c) - \cos(a)\cos(b)}{\sin(a)\sin(b)}$$

The parameters defined here are suited for large scale patterns and do not suffer from projection-induced distortions. They are also independent of symmetries. If the swarm topology is reconstructed

with a symmetry, the parameters of the pattern remain the same. Thus, they can be compared to the ones of the catalog no matter the symmetry.

It is not necessary to compare the measured pattern to every pattern of the catalog. Hence, the catalog size is reduced to its brightest sources. The number of sources remaining is twice the number of measured sources. It is also possible to select only the sources that are brighter than a threshold like it is done for classical star-tracker [8].

A triangle from the list is said to match a triangle from the catalog, if the differences between each of the three parameters are lower than their thresholds. If only one of the three parameters does not meet the required threshold, the triangle does not match. The chosen thresholds suppose that the sources are found within a radius equal to the instrument resolution$\Delta\theta$around their known position. They are defined as follows:

$$\|a_{mes} - a_{cat}\| \leqslant \Delta\Theta$$
$$\|b_{mes} - b_{cat}\| \leqslant \Delta\Theta$$
$$\|\gamma_{mes} - \gamma_{cat}\| \leqslant \Delta\Theta\left(\frac{1}{a_{cat}} + \frac{1}{b_{cat}}\right)$$

This operation generates a table T_{diff} that tells for each triangle made with the measured sources if it matches the triangles of the catalog. An example of this table is depicted in Figure 3a.

The association between a measured source and a source from the catalog is made through a voting system. A similar voting system was implemented by Kolomenkin C. et al [9]. For each pair of sources from the two lists, the algorithm counts the number of matched triangles they share. Each triangle counts as one vote. Summing these votes results in a matrix V whose cells tell the number of votes received for a measured source i (horizontal axis) with a catalog source j (vertical axis) as highlighted in Figure 3b. If two sources match, they should receive numerous votes. On the other hand, if they do not match, they should receive no vote or at least very few.

For instance, if Ns sources are measured and all of them are registered in the catalog (i.e. no false detection), the sources that match should receive (Ns-1)(Ns-2)/2 votes (which is one vote for every possible triangles that include this source) and 0 for the other pairs.

However, in practice, the not matching pairs receive a few votes. In order to discriminate the matching pairs from the other pairs, a threshold is applied on the number of votes. This threshold supposes that at least half of the measured sources have a match in the catalog. It is chosen as: $max(1, (N_s/2 - 1)(N_s/2 - 2))$

Applying this threshold generates a Boolean table $\delta_{i,j}$ (Fig. 3c) that tells if the index i in the list of measured sources corresponds to the same source as the indices j in the catalog.

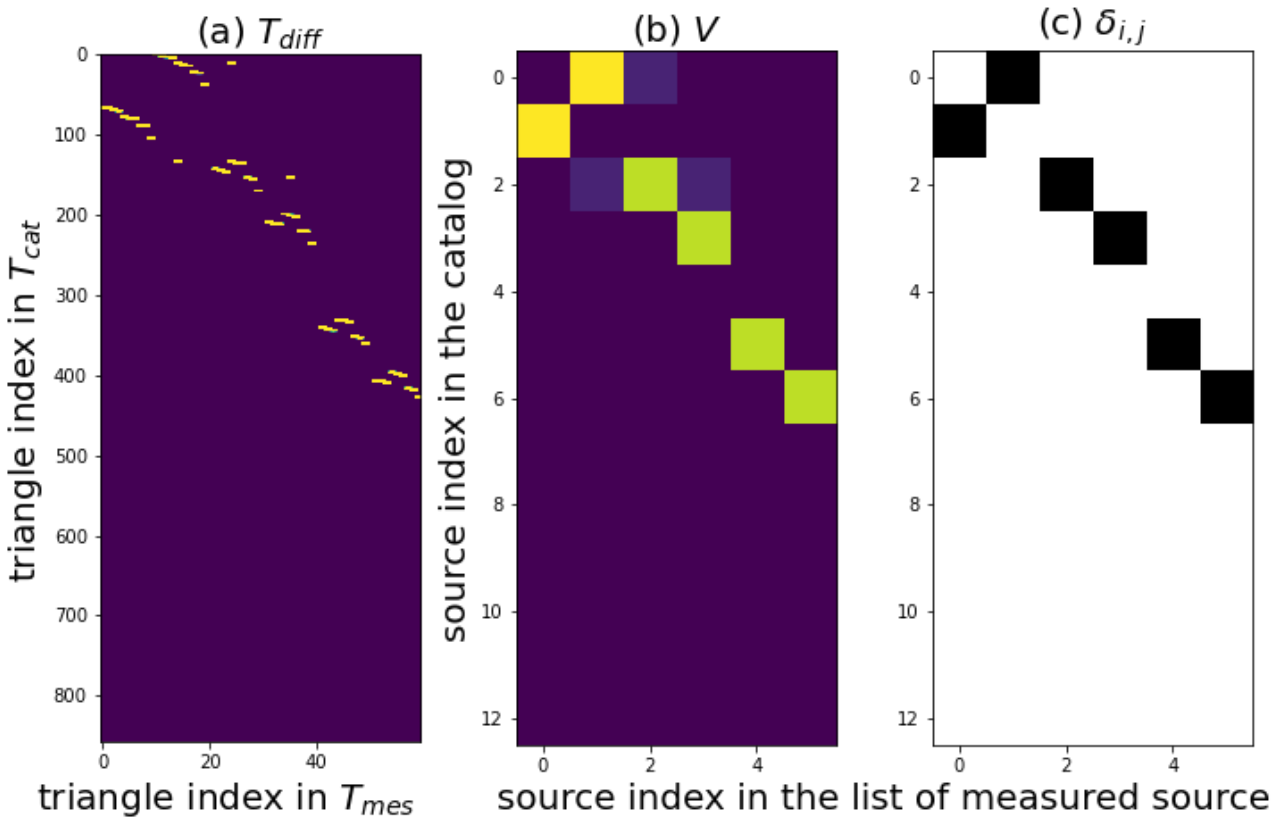

Figure 3: Example of tables generated for the voting method. a) Tdif f, b) V, c) δi,j

These different thresholds are meant to improve the resistance of the pipeline to false detection. Computing the rotation with a false detection or a wrong match would lead to a poor accuracy of the radio-source tracker. The false sources that were not removed during the first selection are then removed of the computation during this process.

2.5 Rotation computation

Once the connection between the found sources and the catalog is made, their positions can be compared. The sources are indexed with the subscript i that refers to the same source in both lists. The rotation matrix$M_{rot}$is computed by minimizing the term below, which is a quadratic sum of angular distances weighted by the brightness of the sources.

$$\sum_i B_i \arccos\left(\overrightarrow{s_{cat,i}}.\left(M_{rot}.\overrightarrow{s_{mes,i}}\right)\right)^2$$

where B_i is the brightness of the source i given by the catalog, $\overrightarrow{s_{cat,i}}$ is the position of the source i on the unit sphere stored in the catalog and $\overrightarrow{s_{mes,i}}$ the measured position of the same source.

This term is minimized twice, with a transform including a symmetry and without. The one that gets best result, i.e. the lowest minimization, is chosen. This operation enables to recover the presence of a symmetry in the transform. It is more reliable than adding a symmetry parameter in the minimization as it is a binary parameter.

3 Stimulation of the pipeline

The pipeline's efficiency is studied by stimulating the pipeline with realistic inputs and by evaluating its outputs with a metric. The individual algorithms are not evaluated on their own, nor they are compared to other algorithms performing the same functions. Only the outputs of the full pipeline are evaluated. For each simulation, the pipeline is stimulated with a different set of inputs

3.1 Stimulation inputs

The swarm of satellites is simulated by a set of points randomly drawn with a uniform distribution inside a sphere of radius 100 km. Their position vectors are supposed to be already expressed in the system frame. The transform between the absolute frame and the system frame is simulated with a random rotation whose angle of rotation is uniformly selected between [-π; π] and whose axis is uniformly selected on the sphere. Also, a symmetry is randomly applied with a fifty-fifty chance to take into account that the reconstruction algorithm may introduce a symmetry. However, in the simulations presented in the result section, the pipeline was not stimulated with symmetries. This transform is applied to the sky before computing the input signal received by the interferometer. This is equivalent to applying the inverse transform to the system frame.

The signal received by the interferometer is simulated using a map of the sky and a list of point sources at 50 MHz that are extrapolated to the frequencies of interest. The extrapolation follows two power laws with a turnover as described by Jester and Falcke [10] for the galaxy. The simulation uses directly the interferometric measurements instead of computing the signals received by every satellite before the interferometric measurements. A random white noise is added to the measurements to account for the noise induced by brightness temperature. The noise amplitude is defined by a dimensionless noise factor noted α. It depends on the acquisition parameters of the instrument and thus can be tuned by the user for the stimulations. It is defined as follow:

$$\alpha = \frac{1}{\sqrt{2\Delta\nu\tau}}$$

where $\Delta\nu$ is the frequency span and τ is the integration time.

3.2 Metric

The Euclidean norm on a rotation matrix is not suited to estimate the offset on the directional information of the images.

For a scientific observation a maximum offset on the imaged field is required. Thus, the figure of interest here is the maximum error. Yet, the offset error measured depends on the position on the celestial sphere.

For now, the precision is evaluated using a Monte-Carlo method: the directional error is evaluated on a set of 1000 vectors uniformly sampled on the unit sphere. The error considered is the maximal value observed over the set of vectors. Both the measured rotation matrix $M_{rot,mes}$ and the simulated rotation $M_{rot,simu}$ are applied to each vector and their angular distance is computed. The maximal offset $\epsilon$is thus computed with:

$$\varepsilon = \underset{\vec{s}\in S^3}{max}\{\ \arccos((M_{rot,mes}.\vec{s}).(M_{rot,simu}.\vec{s}))\ \}$$

The Monte-Carlo method was implemented in order to evaluate the average error in the first place. However, the maximum error is more relevant for the scientific purposes. The method used remains efficient but is not satisfying. A work is in progress to improve it.

4 Results

The results presented here were obtained by averaging the accuracy on multiple runs. The accuracy is evaluated as a function of the noise level for 3 different frequencies: 240 kHz, 400 kHz, 800 kHz. All the simulations were run with the same swarm topology.

Although, the swarm topology impacts the instrumental response, it has shown that it only has a significant influence on the overall accuracy at low level of noise.

On the other hand, the noise draw has a more significant influence over the range of noise factors considered. In order to reduce the influence of the random draws, the accuracy is averaged over 10 simulations with different noise draws.

These results are gathered in Fig 4.

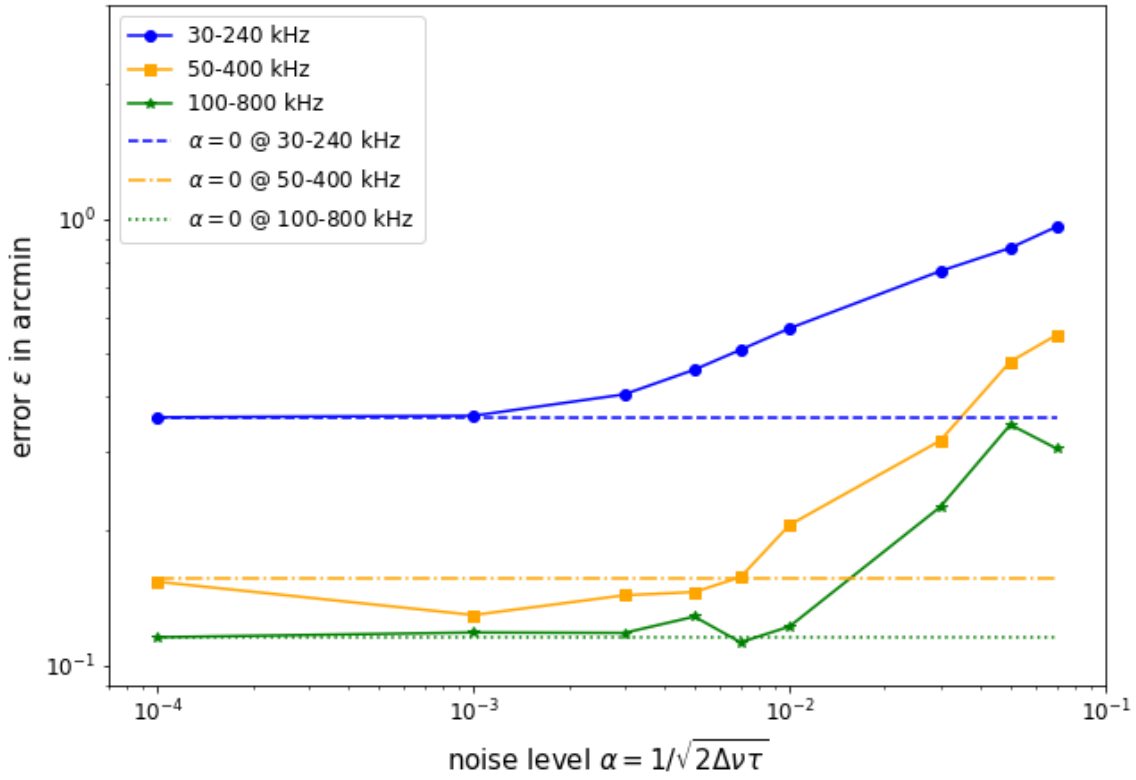

Figure 4: Directional error ε in arcmin as a function of the noise level α for 3 pairs of frequencies

The first result that is outlined by this plot is that the radio-source tracker was able to achieve an accuracy under 1 arcminute in all cases where the noise factor is below 0.1. In comparison, the noise

factor expected for the study solar radio burst is 0.024 with a frequency band of 30 kHz and an integration time of 30 ms.

The plot also highlights how an increase in frequency improves the accuracy. Indeed, for higher frequency, the resolution is enhanced and thus the sources positions are measured with a better accuracy.

On the contrary, the noise decreases the accuracy of the pipeline as it lowers the accuracy on the sources centroids but also because it reduces the number of detected sources. For noise factors above 0.1, it is difficult for the algorithm to detect the sources because of the important noise-induced artifacts. If less than 3 sources are measured, it is impossible for the radio-source tracker to recover the frame transform. That is why no points are plotted for $\alpha > 0.1$, not enough simulations were successful to calculate an average value not biased.

This leads to a lower limit for the acquisition parameters: $\Delta\upsilon\tau > 50$. For example, it corresponds to a frequency band of 1 kHz and an acquisition time of 50 ms.

Although, this is not represented in the figure above, the influence of the symmetry was also evaluated. No differences were noticed with or without it. The pipeline has been successful at discriminating the presence of a symmetry for each simulation.

The random swarm topology has shown to have only a minor sensitivity on the accuracy of the radio-source tracker. It was highlighted that it may permute the order of accuracy among the frequencies at very low level of noise $\alpha < 10^{-3}$. This effect is mostly due to the positions of the main sources relatively to the instrumental response. Hence, for the same geometry but with different orientations relatively to these main sources, the accuracy is different. Also, this effect may be greater for more exotic topology.

5 Discussion

The algorithm pipeline presented in this paper has shown to be able to recover the attitude of the swarm with an accuracy that meets the scientific requirements of NOIRE. The simulations have highlighted a few preliminary constraints on the acquisition parameters. These constraints enable to define the area of use of a radio-source tracker function to recover the absolute attitude.

The results presented here will have to be refined with a proper map of the sky at very low frequency as the simulated sky used for the simulations is extrapolated from the one at 50 MHz. Also, this simulated sky is composed exclusively of extra-solar sources whereas the Sun, the Earth and Jupiter are sources that can emit in the frequency range considered. Simulating these sources could degrades the performances of the radio-source tracker.

With the noise being dominated by brightness temperature, the noise is dependent on the sky brightness. Thus, the lack of information on the sky makes the noise level less representative. Therefore, the maximum noise level that emerged from this study has to be refined as well.

The computation time is generally an important feature for star-trackers. This performance is not regarded in this paper but could be studied in future works. The computation speed for a Lost-In-Space mode has to be evaluated in regard to the angular velocity of the instrument. In the case of an

interferometer, the angular velocity is highly dependent on the topology reconstruction algorithm, which is yet to be implemented and, in addition, it could be designed in way that guarantees stability for the system frame.

Further work is needed to simulate a more realistic sky and also to study the real time implementation of the radio-source tracker. In particular, the tracking mode is yet to be developed while somewhat similar to the LIS mode. Moreover, it would be interesting to study its coupling with the topology reconstruction algorithm and also with a Kalman filter. Such studies will inform, for instance, on the required rate of the tracking mode to ensure a given accuracy.

6 References

[1] Cecconi B. et al., Noire study: Towards a low frequency radio interferometer in space, IEEE Aerospace Conference, 2018.

[2] Kasper J. et al., The sun radio interferometer space experiment (SunRISE) mission concept, IEEE Aerospace, pp. 1-12, 2020.

[3] Xiaogeng Chu and Yuning Chen, Time division inter-satellite link topology generation problem: Modeling and solution, International journal of satellite communications and networking, 194-206, 2018.

[4] Rajan R. and Van Der Veen A., Joint ranging and synchronization for an anchorless network of mobile nodes, IEEE Transactions on signal processing, 1925-1940, 2015.

[5] Duisterwinkel E. et al., Robust reconstruction of sensor swarms floating through enclosed environment, Wireless sensor network, 1-39, 2018.

[6] Gorski et al., HEALPix: A framework for high-resolution discretization and fast analysis of data distributed on the sphere, The astrophysical journal, 759-771, 2005.

[7] C.C. Liebe. Star trackers for attitude determination. IEEE Aerospace and Electronic Systems Magazine, 10–16,1995.

[8] Draper Lawrence T., Star Tracker Calibration, National Aeronautics and Space Administration, Vol. 4594, 1968.

[9] Michael Kolomenkin, et al., Geometric voting algorithm for star trackers. IEEE Transactions on Aerospace and Electronic Systems, 441–456, 2008.

[10] Jester S. and Falcke H., Science with a lunar low-frequency array: From the dark ages of the universe to nearby exoplanets. New Astronomy reviews, 1-26, 2009.